Environ. Sci. Technol. **2011,** *45,* 910–916

Real-Time Methods for Estimating Organic Component Mass Concentrations from Aerosol Mass Spectrometer Data

N. L. NG,[†] M. R. CANAGARATNA,*[,†] J. L. JIMENEZ,[‡,§] Q. ZHANG,[∥] I. M. ULBRICH,[‡,§] AND D. R. WORSNOP[†]

Aerodyne Research, Inc., Billerica, Massachusetts 01821, United States, CIRES and Department of Chemistry and Biochemistry, University of Colorado, Boulder, Colorado 80309, United States, and Department of Environmental Toxicology, University of California, Davis, California 95616, United States

Received August 27, 2010. Revised manuscript received November 22, 2010. Accepted November 30, 2010.

We use results from positive matrix factorization (PMF) analysis of 15 urban aerosol mass spectrometer (AMS) data sets to derive simple methods for estimating major organic aerosol (OA) component concentrations in real time. PMF analysis extracts mass spectral (MS) profiles and mass concentrations for key OA components such as hydrocarbon-like OA (HOA), oxygenated OA (OOA), low-volatility OOA (LV-OOA), semivolatile OOA (SV-OOA), and biomass burning OA (BBOA). The variability in the component MS across all sites is characterized and used to derive standard profiles for real-time estimation of component concentrations. Two methods for obtaining first-order estimates of the HOA and OOA mass concentrations are evaluated. The first approach is the tracer *m*/*z* method, in which the HOA and OOA concentrations are estimated from *m*/*z* 57 and *m*/*z* 44 as follows: HOA $\sim 13.4 \times (C_{57} - 0.1 \times C_{44})$ and OOA $\sim 6.6 \times C_{44}$, where C_i is the equivalent mass concentration of tracer ion *m*/*z i*. The second approach uses a chemical mass balance (CMB) method in which standard HOA and OOA profiles are used as a priori information for calculating their mass concentrations. The HOA and OOA mass concentrations obtained from the first-order estimates are evaluated by comparing with the corresponding PMF results for each site. Both methods reproduce the HOA and OOA concentrations to within ~30% of the results from detailed PMF analysis at most sites, with the CMB method being slightly better. For hybrid CMB methods, we find that fixing the LV-OOA spectrum and not constraining the other spectra produces the best results.

1. Introduction

Organic aerosols (OA) constitute a significant fraction of submicrometer aerosols (*1*) and have important impacts on health, visibility, and climate. Recently, factor analysis of aerosol mass spectrometer (AMS) data has been used to chemically characterize the sources and evolution of OA at many worldwide sites (*1*−*3*). The AMS quantitatively measures and chemically characterizes nonrefractory submicrometer organic aerosols. The OA at most sites can be separated into two main components: hydrocarbon-like OA (HOA) and oxygenated OA (OOA) (*1*). In some sites, biomass burning OA (BBOA) and other local primary OA (POA) can be important contributors to the observed OA loading as well.

HOA components, which on average account for 36% of the observed organic mass in urban sites, show good correlations with primary tracers such as CO, EC, and NO_x (*1, 4*−*6*) and can be considered as surrogates for anthropogenic combustion POA. OOA components, which on average account for 64% of the organic mass in urban areas and 95% of the organic mass in rural/remote regions, correlate with secondary species such as O_3, O_x ($= O_3 + NO_2$), sulfate, and/or nitrate and are considered as surrogates for secondary OA (SOA) (*1, 5*−*8*). The OOA components can include SOA from all sources, such as anthropogenic, biogenic, and biomass burning. OOA can also include gas-phase oxidation products of SVOCs (semivolatile organic compounds) that volatilize from POA and oxidize in the gas phase as well as heterogeneous oxidation products of POA. The OOA component is further resolved into two subtypes that differ in the degree of oxidation and volatility (*2, 3*): low-volatility OOA (LV-OOA) and semivolatile OOA (SV-OOA). Previous work has shown that the simplification of the chemical composition information provided by the AMS organic components can provide key insight necessary for understanding and modeling the evolution of OA in the atmosphere (*1*−*3*).

The main goal of this work is to obtain standardized descriptions of the HOA and OOA component mass spectral (MS) profiles and simple and general parametrizations that can be used for real-time estimation of component concentrations across a wide range of locations. Standard MS profiles can also be used to provide a priori constraints on component source profiles in hybrid source apportionment models (*5*). Individual HOA and OOA component mass spectra and tracer scaling relationships have been previously reported for individual sites (*9, 10*), but the degree of variability in the spectral properties of these components across locations has not been characterized. Thus, in this work the OA components obtained across 15 urban data sets are compared with each other and are used to obtain the standard profiles and tracer scaling relationships. We focus on comparing urban sites because these sites always have contributions from both HOA and OOA components as well as better contrast between their time series which allow for more precise determination of the contributions and MS profiles. Remote sites are often almost completely dominated by OOA and have less time-series contrast and thus are less useful to derive a standard HOA profile.

This manuscript is divided into two parts. First, positive matrix factorization (PMF) analysis results for the urban data sets are described and used to obtain standard MS profiles for HOA, OOA, LV-OOA, SV-OOA, and BBOA components. The standard component profiles are characterized by comparison with reference mass spectra. In the second part of the paper, two real-time methods for estimating HOA and OOA component mass concentrations are evaluated: the tracer *m*/*z* method and the chemical mass balance (CMB) (*11*) based method. Methods for real-time reporting and estimating OA component concentrations are of particular

* Corresponding author phone: (978) 663 9500 × 285, fax: (978) 663 4918, e-mail: mrcana@aerodyne.com.
[†] Aerodyne Research, Inc.
[‡] CIRES, University of Colorado.
[§] Department of Chemistry and Biochemistry, University of Colorado.
[∥] University of California.

10.1021/es102951k

Published on Web 12/27/2010

importance for long-term, remote applications of the AMS, and for aerosol monitoring instruments such as the newly developed Aerodyne aerosol chemical speciation monitor (ACSM) (*12*).

2. Base Case: Positive Matrix Factorization (PMF) Analysis

In this section we use PMF analysis to extract OA components from all data sets. The site-to-site variability in the key mass spectral features of the PMF component spectra is characterized, and individual component spectra are averaged across the multiple data sets to obtain standard HOA, OOA, LV-OOA, SV-OOA, and BBOA component profiles. The OA component mass concentrations obtained from the PMF analysis for each site are then used as the base case against which simpler methods (Section 3: tracer m/z method and CMB method) are evaluated. The PMF results represent a useful base case because they are obtained without any a priori constraints on the OA component profiles.

2.1. Method. Detailed descriptions of the PMF analyses for five of the data sets used here (Beijing, Riverside, Mexico City, Pittsburgh, and Zurich) are available in previous publications (*5, 6, 10, 13, 14*). As part of this work, PMF analyses were performed on each of the remaining data sets (Tokyo summer and winter, Houston, New York City summer and winter, Vancouver, Manchester summer and winter, Mainz, and Edinburgh). These data sets have been analyzed previously with multiple component analysis (MCA) (*1*); however, reanalysis using PMF in this work allows for further deconvolution of the total OOA component reported by Zhang et al. (*1*) into LV-OOA and SV-OOA components. All PMF analyses are based on unit mass resolution (UMR) data.

PMF is a multivariate factor analysis technique developed by Paatero et al. (*15*) to solve the mass conservation problem of pollutant species with the bilinear factor model:

$$x_{ij} = \sum_{p} g_{ip} f_{pj} + e_{ij} \quad (1)$$

where i and j refer to row and column indices in the matrix, respectively, and p is the number of factors in the solution. For AMS data, x_{ij} are the measured concentrations of m/z j in time-step i, reconstructed by p factors having constant source profiles (f_{pj}, factor MS) with varying contributions over the time period of the data set (g_{ip}, factor time series), without any a priori assumptions for either MS or time profiles. e_{ij} are the residuals not fit by the model. PMF computes the solution by minimizing the summed least-squares errors of the fit, weighted with the error estimates of each data point. Solutions are also constrained to have non-negative values. The PMF2 executable version 4.2 is used in robust mode together with a custom software tool for solution comparison and analysis (PMF Evaluation Tool, PET) (*6*). The analysis and input error matrix calculations are performed following the procedures described in (*6*). Further details are also included in the Supporting Information.

2.2. Standard MS Profiles of OA Components. PMF analysis allows for the separation of the OA at all urban sites into HOA and OOA, and sometimes other factors. The mass fractions of the components at each site are shown in Figure S1 (Supporting Information). Overall, OA at most sites are dominated by the OOA component(s); in Beijing, Tokyo (summer), Pittsburgh, Riverside, New York City (summer) and Zurich, the OOA component can be further resolved into LV-OOA and SV-OOA. In addition, a biomass burning factor (BBOA) is also identified in the Mexico City and Houston data sets. Other site-specific local OA factors are also found in some of the data sets.

While they are qualitatively similar, the mass spectra for each of the components display site-to-site variability. The

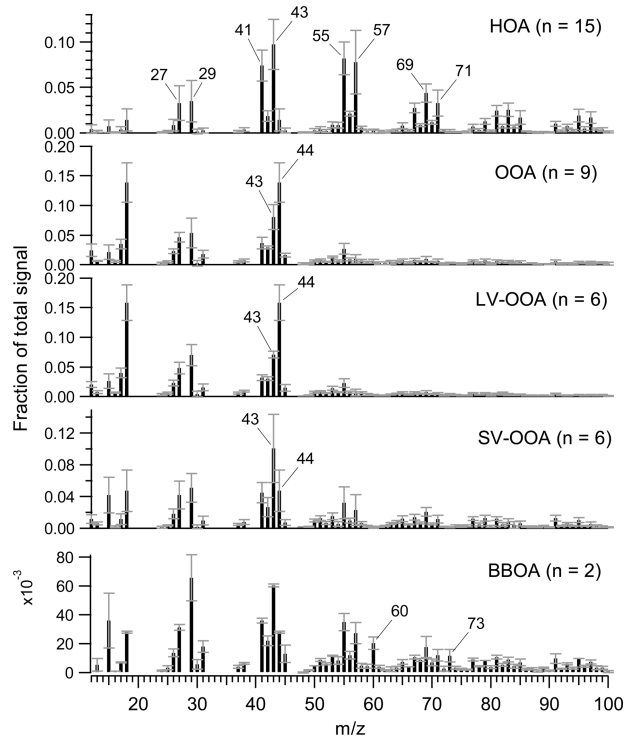

FIGURE 1. Standard mass spectral profiles for HOA, OOA, LV-OOA, SV-OOA, and BBOA components. The error bars represent the variability in each *m/z* fraction (std dev) across all data sets (*n* = number of sites included in the averaging).

"standard profile" for each of the component, which is obtained by averaging together the component mass spectra from all sites, is shown in Figure 1 and tabulated in Table S1 (Supporting Information). The error bars in Figure 1 are the standard deviations in the average "standard profile" intensity at each m/z. The standard HOA profile is distinguished and dominated by alkyl fragment signatures. The $C_nH_{2n+1}^+$ ion series (m/z 29, 43, 57, 71, 85, 99...) accounts for 27% of the HOA signal and the $C_nH_{2n-1}^+$ (m/z 27, 41, 55, 69, 83, 97...) ion series accounts for 28%. The key feature of all OOA components is the presence of a prominent m/z 44 (CO_2^+) peak. The standard OOA, LV-OOA, and SV-OOA profiles have average f_{44} (ratio of m/z 44 to total signal in the component MS, same notation used for other m/z below) of 0.14, 0.16, and 0.05, respectively. For comparison, HOA has an average f_{44} of 0.01. LV-OOA has higher f_{44} and thus is more oxidized (i.e., has higher estimated O:C) than SV-OOA. Previous characterization of worldwide OOA components has shown a wide range of O:C for both SV-OOA and LV-OOA that converges to highly oxidized LV-OOA with photochemical aging (*2, 3, 16*). The standard total OOA and LV-OOA profiles (obtained from sites with one or two subtypes of OOA, respectively) are very similar to each other ($R^2 = 0.99$) while the standard total OOA and SV-OOA profiles are more different ($R^2 = 0.66$), suggesting that at the sites where only total OOA is identified this component is dominated by aged regional SOA with relatively little fresh SOA contribution.

Only in two of the sites (Mexico City and Houston) was BBOA identified explicitly as an OA component. Thus, the standard BBOA profile may not fully represent the variability that can be observed in BBOA impacting urban sites. The majority of the ions in the standard BBOA profile are similar to those found in both the standard HOA and OOA profiles. The distinguishing feature of the BBOA spectrum is the presence of ion signals at m/z 60 ($C_2H_4O_2^+$) and 73 ($C_3H_5O_2^+$), which are known to be produced by levoglucosan, a tracer of biomass burning and related species (*17*). It is noted that the f_{44} of the BBOA component (0.03) is higher than that in

the HOA component (0.01), indicating that the BBOA component has higher O:C than HOA, consistent with direct measurements (*10*).

As mentioned earlier, HOA is a surrogate of OA produced from various anthropogenic combustion POA sources, and OOA is a surrogate of SOA produced from multiple sources. Since the standard profiles are obtained as an average from sites with different primary and secondary source influences, the generality of the standard profile is evaluated by comparing with several types of reference MS from primary and secondary sources (AMS mass spectra database: http://cires.colorado.edu/jimenez-group/AMSsd/). The data include direct source measurements (primary references) (*18, 19*) and ambient measurements over well-defined periods characteristic of mixed-source or biogenic-dominated SOA (*20, 21*). The standard HOA profile has higher similarity (R^2 = 0.85−0.99) to anthropogenic combustion POA sources such as lubricating oil, diesel exhaust, diesel fuel, and cooking aerosols, with a substantially lower correlation with other POA sources such as reference BBOA (R^2 = 0.33−0.70) and even lower for reference SOA (R^2 = 0.06−0.26). This indicates that the standard HOA profile is representative of nonbiomass burning related mixed anthropogenic POA in ambient environments. Component mass concentrations estimated from the standard HOA profile could, for example, be used to quantify and map the evolution of vehicular source PM as it is diluted and processed after emission into ambient environments (*22*). The standard LV-OOA and total OOA profiles correlate better with SOA MS (R^2 = 0.90−0.98) than all combustion POA reference MS (R^2 = 0.08−0.53) or reference BBOA MS (R^2 = 0.28−0.86). This indicates that standard OOA and LV-OOA profiles will be useful for apportionment of SOA, especially for environments/time periods which are not affected by more oxidized BBOA. The fact that the standard LV-OOA and OOA profiles display the same degree of correlation with the biogenically and anthropogenically influenced reference SOA MS indicates that they do not distinguish between these specific sources of SOA.

The standard BBOA profile correlates the best with reference BBOA spectra (R^2 = 0.57−0.91), and less well with HOA and SOA references. The standard SV-OOA profile has similar correlation coefficients with most of the reference spectra, although the best correlation is with the fresher biogenic SOA MS. This reflects the fact that in general the SV-OOA components have both OOA and HOA-type features and higher spectral variability. Taken together these results indicate that source apportionment analyses based on fixed standard MS profiles for SV-OOA and BBOA may be ambiguous and may require further constraints of source profiles or full PMF analysis.

2.3. Ratios of OA Components to External Tracers. Component time trends and correlations with external tracers provide essential information for relating OA components to their sources. The slopes obtained when comparing time trends of the individual components and some of the key tracers (CO, nitrate, and sulfate) are shown in Table S2 (Supporting Information). CO, which is a tracer of combustion, correlates well with HOA. Aerosol nitrate and sulfate, on the other hand, are tracers of secondary aerosol formation and tend to correlate with more volatile and less volatile SOA components, respectively (*2, 5, 6*). We compile together a range of "OA component to tracer" ratios. For the sites included in this study, the ranges for the HOA/ΔCO, LV-OOA/sulfate, and SV-OOA/nitrate ratios are 2.4−9.1 $\mu g/m^3$/ppm, 0.27−0.57, and 0.10−1.42, respectively. In general, the LV-OOA components correlate better with sulfate, and the SV-OOA components correlate better with nitrate (Figure S3a, Supporting Information), consistent with previous studies (*2, 5, 6*). This behavior is consistent with the assignment of SV-OOA components as fresher and semivolatile and LV-OOA components as aged and of low volatility. Figure S3b shows further evidence for the aerosol loading-dependent partitioning of OOA (total OOA) in ambient aerosol (*3*). The data points correspond to periods when partitioning of semivolatiles is expected (i.e., in the mornings when the temperature is lower and there is a larger change in temperature). Taken together, the data show a general decrease in f_{44} with increasing organics loadings. This behavior is consistent with the partitioning of semivolatiles (*23, 24*).

2.4. Spectral Variability of AMS Tracer Ions. Tracer ions are distinctive ion fragments in each OA component whose signal level correlates strongly with the total concentration of that component and thus can be used to approximate OA component concentrations even if they account for only a small fraction of that component's total mass (*9, 10*). Figure 2 shows the relative MS intensity and variability of potential tracer fragments (m/z with typically high signal levels in some OA spectra: 27, 29, 43, 44, 55, 57, 60, 73, 77, 91) in standard profiles and reference spectra. Figure 2 confirms that the most unambiguous tracer for OOA components and secondary aerosol is m/z 44, due to the combination of high f_{44} values in OOA and SOA (average value = 0.13 and 0.14, respectively) and low values for most POA sources. Although m/z 57 is present in many of the components, it is much higher in the HOA components and combustion POA reference MS; the average value of f_{57} in the HOA and POA reference spectra are 0.07 and 0.08. The much lower values of f_{57} in OOA, SOA (∼0.01), and BBOA (∼0.03) make it the most distinctive HOA tracer. f_{55} shows a similar pattern to f_{57} but the contrast between POA and the other sources is smaller and thus is not as good of an HOA tracer. However, f_{55} appears to be enhanced in cooking aerosol (*14, 25*) and so it may be a useful tracer for that source. BBOA components and BBOA reference spectra show very elevated f_{60} and f_{73} when compared to the other sources/components. There is substantial variability in f_{60} and f_{73} of the BBOA reference spectra used here, which contrasts with the remarkably constant values of f_{60} reported by Lee et al. (*17*) who examined a wider range of biomasses. Given these conflicting results, caution is recommended when using the tracer approach to estimate BBOA.

Previous studies have suggested that mass spectral fragments 27 ($C_2H_3^+$) and 29 ($C_2H_5^+$) may be tracers of biogenic SOA (*18*). m/z 29 is also often an intense fragment in BBOA. The average f_{27} values are similar across all the components and reference spectra, indicating that it is not a useful tracer for any particular OA component. f_{29} in BBOA is larger than in HOA but is similar to OOA values, which limits its value as a tracer. Due to contributions from both oxygenated and reduced ions to m/z 43 ($C_3H_7^+$ and $C_2H_3O^+$), f_{43} has about the most constant values across all OA components, and thus it is rather a useful tracer of total OA (*25*). The mass fragments m/z 77 ($C_6H_5^+$) and 91 ($C_7H_7^+$) can arise from fragmentation of aromatic compounds (*26*) but can also arise in α-pinene SOA (*27*). Neither f_{77} nor f_{91} shows a distinctive pattern across the components or reference spectra, limiting their usefulness as tracers.

3. Real-Time Estimates of OA Component Concentrations

3.1. Tracer *m/z* Method. In this method, linear combinations of tracer ion fragments are used to estimate OA component concentrations. As shown above, m/z 44, m/z 57, and m/z 60 are distinctive tracers for OOA, HOA, and BBOA, respectively. Here we use the urban site data to determine the tracer scaling factors for reproducing the HOA and OOA concentrations (results from PMF analysis) from these ions. Since

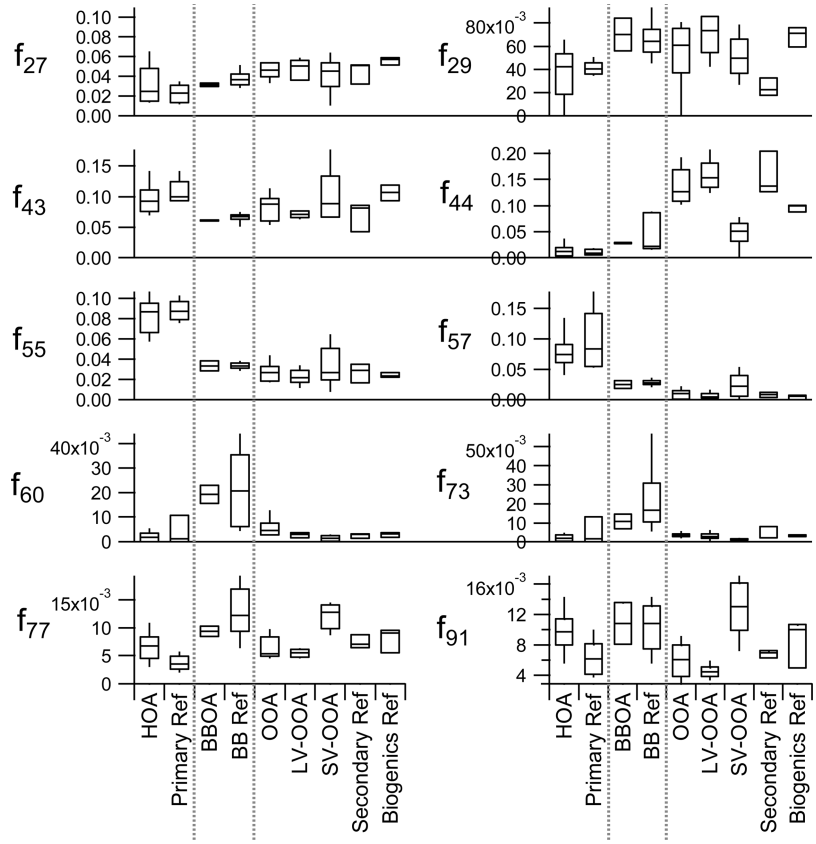

FIGURE 2. Average value and variability of relative intensities of important mass fragments (*m/z* 27, 29, 43, 44, 55, 57, 60, 73, 77, 91) in OA component spectra at each site, as well as for reference MS.

BBOA was only identified in two studies, we do not pursue its estimation further.

For each site, a tracer scaling factor is obtained as the slope of the fit between the PMF time series of the component and the time series (i.e., equivalent mass concentration) of its tracer ion i (C_i). For this analysis, total OOA is estimated from C_{44}. High resolution spectral analysis by Aiken et al. (*10*) has shown that the m/z 57 ion fragment is dominated by a reduced ion ($C_4H_9^+$) from HOA but also can contain non-negligible contribution from an oxygenated fragment ($C_3H_5O^+$) of OOA. Aiken et al. (*10*) proposed to estimate HOA and OOA based on:

$$\mathrm{HOA_{est}} = b\mathrm{x}(C_{57} - a\mathrm{x}C_{44}) \quad (2)$$

$$\mathrm{OOA_{est}} = c\mathrm{x}C_{44} + d \quad (3)$$

The last term in eq 2 accounts for the contribution of OOA to m/z 57 and thus a is the ratio of m/z 57 to m/z 44 in the OOA component spectrum for that site. Aiken et al. (*10*) determined that $a = 0.1$ based on HR component spectra and that b, c, d (for Mexico City data) are 16, 9, and −5.3 μg/m^3, respectively. The values of a for the OOA components in this study are also found to be around 0.1 for most sites, and the values of d are <0.3 μg/m^3 for all sites (Beijing has a value of 0.78 μg/m^3 and is treated as an outlier). The values and fitting errors of a, b, c, and d for each site can be found in Table S3 (Supporting Information). The fitting errors in the parameters are generally much smaller for individual sites than the variation in these parameters between sites.

Figure 3a and 3b shows the values of b and c calculated from eq 2 and eq 3 for the HOA and OOA components at each site. For HOA, $b = 13.4 \pm 3.3$ (range 8.5−19.2). The Beijing data is regarded as an outlier and excluded when calculating the average value. The variability in the observed scaling factors may be related to different mixtures of primary

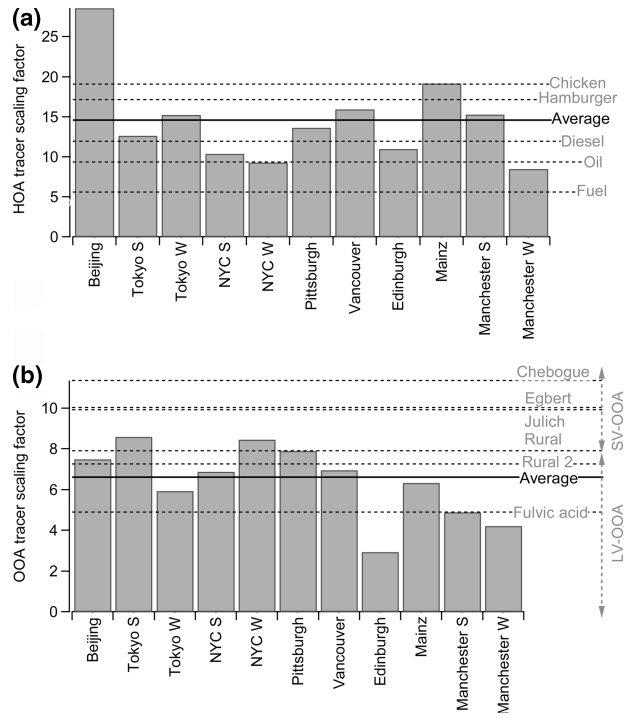

FIGURE 3. Tracer scaling factors for (a) HOA and (b) OOA at each site. The black solid line shows the average values from all sites. The black dashed lines show the estimated scaling factors for the reference mass spectra. "S" and "W" denote "summer" and "winter", respectively.

combustion and other reduced OA sources in the different sites. The scaling factors for HOA reference MS (those shown in Figure S2, Supporting Information) are also shown in Figure

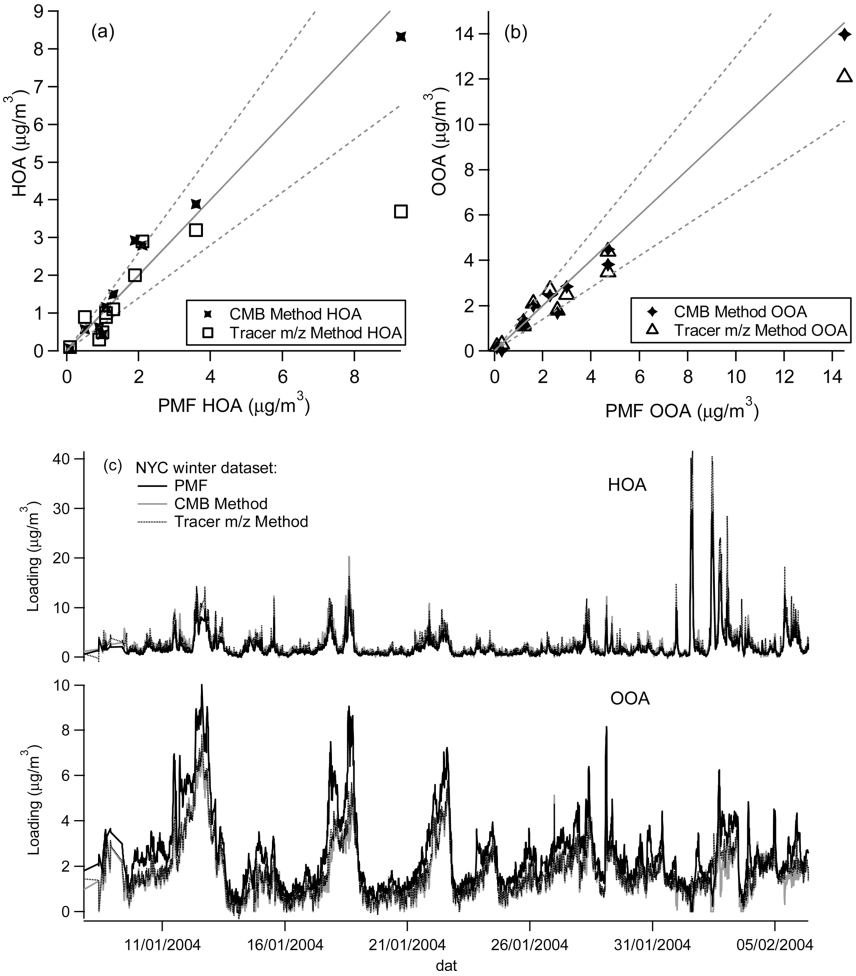

FIGURE 4. Estimated (a) HOA and (b) OOA concentrations from the tracer *m/z* and CMB methods vs the results of PMF analysis. Solid line is the 1:1 line, dotted lines are ±30% from the 1:1 line. (c) Time series of HOA and OOA from the New York City winter data set determined from PMF analysis and estimated from the tracer *m/z* and CMB methods.

3a (calculated simply as $1/f_{57}$ since the contribution of the secondary oxygenated ions to m/z 57 is negligible). The reference MS scaling factors span the same range of the HOA components observed. The tracer scaling factor of the Beijing data set is close to those of the reference cooking MS, consistent with the fact that there are large contributions from cooking POA in the Beijing data set (*14*). However, currently, we do not have sufficient information to suggest a one-to-one correspondence between scaling factor values and source dominance. The source dependence of the HOA tracer scaling factors should be studied further in the future when more data sets are available, especially high-resolution data sets. For OOA, $c = 6.6 \pm 1.9$ (range 2.9−9.0). Also shown in Figure 3b are the values of c for OOA reference MS ($= 1/f_{44}$). The LV- and SV-OOA ranges are from Ng et al. (*3*), which also included PMF analysis at rural and remote sites which are typically dominated by OOA.

The accuracy of tracer scaling relationships in predicting component concentrations is evaluated by calculating the concentrations of HOA and OOA components from the average values of the scaling factors determined above (with $b = 13.4$, $a = 0.1$, $c = 6.6$, and $d = 0$) and comparing them with the concentrations determined from PMF analysis. As shown in Figure 4a, these average tracer scaling factors provide estimations of average OA component concentrations that are within ~30% of the PMF results for most sites. The tracer-based estimations also provide useful time trends of the components at all sites, as shown in Figure 4c for the New York City-winter data set. The R^2 of the tracer-estimated and PMF time series ranges from 0.67 to 0.97.

3.2. Chemical Mass Balance (CMB) Method. The mathematical model of CMB, which is the same eq 1 as shown above for PMF, expresses mass conservation in terms of pollutant sources with constant composition profiles. The key difference is that in CMB the source profiles (component MS) are prescribed before the analysis, rather than derived from the data matrix as in PMF. CMB can be applied for real-time estimation of OA component concentrations, by expressing the observed mass spectrum at each time step as a linear combination of standard component MS and finding the component contributions that minimize the differences between the total measured and reconstructed MS. A linear least-squares fitting procedure (from Igor Pro 6.12A, WaveMetrics Inc.) is used to fit each time step separately. CMB has not been applied previously to AMS data to our knowledge.

In this work, the standard profiles obtained above are used as fixed source profiles for all data sets. Three different combinations of the standard profiles are evaluated: (1) HOA and OOA. (2) HOA and LV-OOA. The residual of the fit is regarded as SV-OOA for sites with such a component. (3) HOA, LV-OOA, and SV-OOA. CMB analysis with the standard HOA and OOA profiles as inputs results in a better estimation of the total OA concentration compared to the other two combinations. For sites with both LV-OOA and SV-OOA components, the times series of the SV-OOA component is not well-retrieved using the latter two combinations mentioned above. This is consistent with the higher variability of the SV-OOA component spectra across sites. As seen in Figure 4b, the concentrations estimated from the first

combination agree within ~30% with the PMF results. The estimated component time series also follow the PMF trends fairly well (Figure 4c). The R^2 of the CMB-estimated and PMF time series is >0.90 for almost all sites.

The sensitivity of the analysis to variations in the source profiles is explored with randomly generated HOA and OOA component spectral profiles. The New York City-summer data set is used as a case study for these calculations. In the first scenario, the standard HOA profile and a randomly generated OOA MS profile are used as CMB inputs. For the randomly generated OOA MS, the intensity at each m/z is allowed to vary within the appropriate standard deviation for that m/z in the standard OOA MS profile. Fits are performed separately for 150 different OOA MS profiles. In the second scenario, the standard OOA profile and 150 randomly generated HOA MS profiles (allowing each m/z to vary within the standard deviation of the standard HOA MS) are used as inputs. These simulations show that mass spectra within the standard deviations of the standard profiles still reproduce the HOA and OOA concentrations to within ~30% of those obtained from PMF analysis. Results from these simulations are shown in Figure S3.

While the discussion above has focused on real-time estimates, the standard spectra can also be used for post-processing with hybrid factor analysis. These methods incorporate aspects of both PMF and CMB: they involve solving eq 1 by fitting the whole data matrix (i.e., a compilation of mass spectra at *all* times) simultaneously while imposing some partial constraints on the MS of some components. In this work, the hybrid CMB modeling was performed using the Multilinear Engine (ME2) tool (*4*) as described in Lanz et al. (*5*). In this hybrid CMB model analyses, eq 1 is expressed in terms of HOA, LV-OOA, and SV-OOA components, and simple constraints on the component MS are tested. Table S4 (Supporting Information) shows results from (1) fixing all three component MS to their standard profiles and (2) fixing only HOA or only LV-OOA MS to their standard profiles while allowing the other two-component MS to vary from starting values corresponding to their standard profiles. For the first case, the component concentrations are reproduced to within 30% of the detailed PMF analysis. For the second case, the total OOA and HOA mass concentrations are best reproduced when the LV-OOA component MS rather than the HOA component MS is fixed to the standard profile values. When only the LV-OOA component MS is fixed to its standard profile values, however, the relative split between LV-OOA and SV-OOA is not well reproduced. More data sets need to be analyzed to evaluate the use of the standard profiles in these analyses.

Acknowledgments

We acknowledge grants NSF ATM-0449815 and ATM-0919189, DOE (BER, ASR Program) DEFG0208ER64627, NOAA NA08OAR4310565, EPA STAR-R833747, and NASA and CIRES fellowships for IMU for partial support of this work.

Supporting Information Available

Additional analysis results including supplementary figures and tables. This material is available free of charge via the Internet at http://pubs.acs.org.

Literature Cited

(1) Zhang, Q.; Jimenez, J. L.; Canagaratna, M. R.; Allan, J. D.; Coe, H.; Ulbrich, I.; Alfarra, M. R.; Takami, A.; et al. Ubiquity and dominance of oxygenated species in organic aerosols in anthropogenically-influenced Northern Hemisphere midlatitudes. *Geophys. Res. Lett.* **2007**, *34*, L13801. Doi: 13810.11029/12007GL029979.

(2) Jimenez, J. L.; Canagaratna, M. R.; Donahue, N. M.; Prevot, A. S. H.; Zhang, Q.; Kroll, J. H.; DeCarlo, P. F.; Allan, J. D.; et al. Evolution of Organic Aerosols in the Atmosphere. *Science* **2009**, *326*, 1525–1529.

(3) Ng, N. L.; Canagaratna, M. R.; Zhang, Q.; Jimenez, J. L.; Tian, J.; Ulbrich, I. M.; Kroll, J. H.; Docherty, K. S.; et al. Organic aerosol components observed in worldwide datasets from aerosol mass spectrometry. *Atmos. Chem. Phys.* **2010**, *10*, 4625–4641.

(4) Zhang, Q.; Worsnop, D. R.; Canagaratna, M. R.; Jimenez, J. L. Hydrocarbon-like and oxygenated organic aerosols in Pittsburgh: insights into sources and processes of organic aerosols. *Atmos. Chem. Phys.* **2005**, *5*, 3289–3311.

(5) Lanz, V. A.; Alfarra, M. R.; Baltensperger, U.; Buchmann, B.; Hueglin, C.; Prévôt, A. S. H. Source apportionment of submicron organic aerosols at an urban site by factor analytical modelling of aerosol mass spectra. *Atmos. Chem. Phys.* **2007**, *7*, 1503–1522.

(6) Ulbrich, I. M.; Canagaratna, M. R.; Zhang, Q.; Worsnop, D. R.; Jimenez, J. L. Interpretation of organic components from Positive Matrix Factorization of aerosol mass spectrometric data. *Atmos. Chem. Phys.* **2009**, *9*, 2891–2918.

(7) de Gouw, J. A.; Middlebrook, A. M.; Warneke, C.; Goldan, P. D.; Kuster, W. C.; Roberts, J. M.; Fehsenfeld, F. C.; Worsnop, D. R.; et al. Budget of organic carbon in a polluted atmosphere: Results from the New England Air Quality Study in 2002. *J. Geophys. Res.-Atmos.* **2005**, *110*, D16305. Doi: 16310.11029/12004JD005623.

(8) Herndon, S. C.; Onasch, T. B.; Wood, E. C.; Kroll, J. H.; Canagaratna, M. R.; Jayne, J. T.; Zavala, M. A.; Knighton, W. B.; et al. Correlation of secondary organic aerosol with odd oxygen in Mexico City. *Geophys. Res. Lett.* **2008**, *35*, L15804. Doi: 15810.11029/12008GL034058.

(9) Zhang, Q.; Alfarra, M. R.; Worsnop, D. R.; Allan, J. D.; Coe, H.; Canagaratna, M. R.; Jimenez, J. L. Deconvolution and quantification of hydrocarbon-like and oxygenated organic aerosols based on aerosol mass spectrometry. *Environ. Sci. Technol.* **2005**, *39*, 4938–4952.

(10) Aiken, A. C.; Salcedo, D.; Cubison, M. J.; Huffman, J. A.; DeCarlo, P. F.; Ulbrich, I. M.; Docherty, K. S.; Sueper, D.; et al. Mexico City aerosol analysis during MILAGRO using high resolution aerosol mass spectrometry at the urban supersite (T0) - Part 1: Fine particle composition and organic source apportionment. *Atmos. Chem. Phys.* **2009**, *9*, 6633–6653.

(11) Schauer, J. J.; Rogge, W. F.; Hildemann, L. M.; Mazurek, M. A.; Cass, G. R. Source apportionment of airborne particulate matter using organic compounds as tracers. *Atmos. Environ.* **1996**, *30*, 3837–3855.

(12) Ng, N. L.; Herndon, S. C.; Trimborn, A.; Canagaratna, M. R.; Croteau, P.; Onasch, T. M.; Sueper, D.; Worsnop, D. R. et al. An Aerosol Chemical Speciation Monitor (ACSM) for routine monitoring of atmospheric aerosol composition. *Aerosol Sci. Technol.* **2010**, submitted.

(13) Docherty, K. S.; Stone, E. A.; Ulbrich, I. M.; DeCarlo, P. F.; Snyder, D. C.; Schauer, J. J.; Peltier, R. E.; Weber, R. J.; et al. Apportionment of Primary and Secondary Organic Aerosols in Southern California during the 2005 Study of Organic Aerosols in Riverside (SOAR-1). *Environ. Sci. Technol.* **2008**, *42*, 7655–7662.

(14) Sun, J.; Zhang, Q.; Canagaratna, M. R.; Zhang, Y.; Ng, N. L.; Sun, Y.; Jayne, J. T.; Zhang, X.; et al. Highly Time- and Size-Resolved Characterization of Submicron Aerosol Particles in Beijing Using an Aerodyne Aerosol Mass Spectrometer. *Atmos. Environ.* **2010**, 131–140.

(15) Paatero, P.; Tapper, U. Positive Matrix Factorization - a Nonnegative Factor Model with Optimal Utilization of Error-Estimates of Data Values. *Environmetrics.* **1994**, *5*, 111–126.

(16) Morgan, W. T.; Allan, J. D.; Bower, K. N.; Highwood, E. J.; Liu, D.; McMeeking, G. R.; Northway, M. J.; Williams, P. I.; et al. Airborne measurements of the spatial distribution of aerosol chemical composition across Europe and evolution of the organic fraction. *Atmos. Chem. Phys.* **2010**, *10*, 4065–4083.

(17) Lee, A.; Sullivan, A. P.; Mack, L.; Jimenez, J. L.; Kreidenweis, S. M.; Onasch, T. B.; Worsnop, D. R.; Malm, W. et al. Variation of chemical smoke marker emissions during flaming vs. smoldering phases of laboratory open burning of wildland fuels. *Aerosol Sci. Technol.* **2010**, in press.

(18) Schneider, J.; Weimer, S.; Drewnick, F.; Borrmann, S.; Helas, G.; Gwaze, P.; Schmid, O.; Andreae, M. O.; et al. Mass spectrometric analysis and aerodynamic properties of various types of combustion-related aerosol particles. *Int. J. Mass Spectrom.* **2006**, *258*, 37–49.

(19) Canagaratna, M. R.; Jayne, J. T.; Ghertner, D. A.; Herndon, S.; Shi, Q.; Jimenez, J. L.; Silva, P. J.; Williams, P.; et al. Chase studies of particulate emissions from in-use New York City vehicles. *Aerosol Sci. Technol.* **2004**, *38*, 555–573.

(20) Kiendler-Scharr, A.; Zhang, Q.; Hohaus, T.; Kleist, E.; Mensah, A.; Mentel, T. F.; Spindler, C.; Uerlings, R.; et al. Aerosol Mass Spectrometric Features of Biogenic SOA: Observations from a Plant Chamber and in Rural Atmospheric Environments. *Environ. Sci. Technol.* **2009**, *43*, 8166–8172.
(21) Slowik, J. G.; Stroud, C.; Bottenheim, J. W.; Brickell, P. C.; Chang, R. Y. W.; Liggio, J.; Makar, P. A.; Martin, R. V.; et al. Characterization of a large biogenic secondary organic aerosol event from eastern Canadian forests. *Atmos. Chem. Phys.* **XXX**, *10*, 2825–2845.
(22) Canagaratna, M. R.; Onasch, T. B.; Wood, E. C.; Herndon, S. C.; Jayne, J. T.; Cross, E. S.; Miake-Lye, R. C.; Kolb, C. E.; et al. Evolution of vehicle exhaust particles in the atmosphere. *J. Air Waste Manage. Assoc.* **2010**, *60*, 1192–1203.
(23) Odum, J. R.; Hoffmann, T.; Bowman, F.; Collins, D.; Flagan, R. C.; Seinfeld, J. H. Gas/particle partitioning and secondary organic aerosol yields. *Environ. Sci. Technol.* **1996**, *30*, 2580–2585.
(24) Donahue, N. M.; Robinson, A. L.; Stanier, C. O.; Pandis, S. N. Coupled partitioning, dilution, and chemical aging of semivolatile organics. *Environ. Sci. Technol.* **2006**, *40*, 2635–2643.
(25) Mohr, C.; Huffman, J. A.; Cubison, M. J.; Aiken, A. C.; Docherty, K. S.; Kimmel, J. R.; Ulbricht, I. M.; Hannigan, M.; et al. Characterization of Primary Organic Aerosol Emissions from Meat Cooking, Trash Burning, and Motor Vehicles with High-Resolution Aerosol Mass Spectrometry and Comparison with Ambient and Chamber Observations. *Environ. Sci. Technol.* **2009**, *43*, 2443–2449.
(26) McLafferty, L. W.; Turecek, F. *Interpretation of Mass Spectra.*; University Science Books: Mill Valley, CA, 1993.
(27) Shilling, J. E.; Chen, Q.; King, S. M.; Rosenoern, T.; Kroll, J. H.; Worsnop, D. R.; DeCarlo, P. F.; Aiken, A. C.; et al. Loading-dependent elemental composition of alpha-pinene SOA particles. *Atmos. Chem. Phys.* **2009**, *9*, 771–782.

ES102951K